



Using data on soil ECa, soil water properties, and response of tree root system for spatial water balancing in an apple orchard

Nikos Tsoulias^{1,2} · Robin Gebbers¹ · Manuela Zude-Sasse¹

Published online: 9 August 2019

© Springer Science+Business Media, LLC, part of Springer Nature 2019

Abstract

The study aims at spatial analysis of water deficit of fruit trees under semi-humid climate conditions. Differences of soil, root, and their relation with the spatial variability of crop evapotranspiration (ET_a) were analyzed. Measurements took place in a six hectare apple orchard (*Malus x domestica* ‘Gala’) located in fruit production area of Brandenburg (latitude: 52.606°N, longitude: 13.817°E). Data of apparent soil electrical conductivity (ECa) in 25 cm were used for guided sampling of soil texture, bulk density, rooting depth, root water potential, and volumetric water content. Soil ECa showed high correlation with root depth. The readily available soil water content (RAW) was calculated considering three cases utilizing (i) uniform root depth of 1 m, (ii) measured values of root depth, and (iii) root water potential measured during full bloom, fruit cell division stage, at harvest. The RAW set the thresholds for irrigation. The ET_a was calculated based on data from a weather station in the field and RAW cases in high, medium and low ECa conditions. ET_a values obtained were utilized to quantify how fruit trees cope with spatial soil variability. The RAW-based irrigation thresholds for locations of low and high ECa value differed. The implementation of plant parameters (rooting depth, root water potential) in the water balance provided a more representative figure of water needs of fruit trees. Consequently, the precise adjustment of irrigation including plant data can optimize the water use.

Keywords Irrigation · Root depth · Root water potential · Perennial · Precision horticulture

Abbreviations

D_e	Daily cumulative depth of water depleted from the surface (mm)
$D_{r,i}$	Water depletion in the root zone at the end of day i (mm)
DP_i	Water loss out of the root zone by deep percolation on day i (mm)
$DP_{e,i}$	Water loss from the top soil by deep percolation at the end of day i (mm)
e_s	Saturation vapour pressure (kPa)

✉ Manuela Zude-Sasse
mzude@atb-potsdam.de

¹ Leibniz Institute for Agricultural Engineering and Bioeconomy, Max-Eyth-Allee 100, 14469 Potsdam, Germany

² Department of Natural Resources Management & Agricultural Engineering, Agricultural University of Athens, Iera Odos 75, 118 55 Athens, Greece

e_a	Actual vapour pressure (kPa)
E_i	Evaporation at the end of day i (mm)
ECa	Apparent soil electrical conductivity (mS/m)
ET_0	Reference evapotranspiration (mm)
ET_a	Actual crop evapotranspiration (mm)
$ET_{a,RF}$	Actual crop evapotranspiration adjusted to soil texture and plant height considering mean root depth of 1 m
$ET_{a,RD}$	Actual crop evapotranspiration adjusted to soil texture and plant height considering variable root depth (mm)
$ET_{a,\Psi}$	Crop evapotranspiration adjusted to soil texture and plant height considering variable root depth and root water potential (mm)
$f_{ew,i}$	The daily exposed and wetted soil fraction (Allen et al. 1998)
f_w	The fraction of wetted soil surface (Allen et al. 1998)
h	Mean tree height (m)
I	Irrigation (mm)
G	Soil heat flux (MJ/m^2 days)
K_{cb}	Basal crop coefficient
$K_{cb,ini}$	Initial basal crop coefficient during bud break and end full bloom, adjusted to field conditions
$K_{cb,mid}$	Basal crop coefficient during full bloom and beginning of harvest, adjusted to field conditions
$K_{cb,end}$	Basal crop coefficient during harvest till defoliation, adjusted to field conditions
$K_{cb,max}$	Maximum value of basal crop coefficient during the cultivation period, adjusted to field conditions
$K_{c,ini}$ (tab)	Initial crop coefficient according to Table 12 (Allen et al. 1998)
$K_{c,mid}$ (tab)	Midterm crop coefficient according to Table 12 (Allen et al. 1998)
$K_{c,end}$ (tab)	Crop coefficient after harvest according to Table 12 (Allen et al. 1998)
$K_{e,RF,RD}$	Soil surface evaporation coefficient
$K_{e,\Psi}$	Soil surface evaporation coefficient based on measured values
$K_{r,RF,RD}$	Soil evaporation reduction coefficient (Allen et al. 1998)
$K_{r,\Psi}$	Soil evaporation reduction coefficient based on measured values
$K_{s,RF}$	Soil water stress coefficient adjusted to soil texture $K_{s,RD}$ Soil water stress coefficient adjusted to soil texture and variable root depth
$K_{s,\Psi}$	Soil water stress coefficient adjusted to soil texture, variable root depth and midday root water potential (mm)
p	The average fraction of TAW that can be depleted from the root zone before the revealing of moisture stress (mm)
p_{tab}	Tabulated p values (Allen et al. 1998)
P	Precipitation (mm)
RAW_{RF}	Readily available water content in the root zone adjusted to soil texture and tree height (mm)
RAW_{RD}	Readily available water content in the root zone adjusted to soil texture, tree height, and variable root depth measured (mm)
RAW_{Ψ}	Readily available water content in the root zone adjusted to soil texture, variable root depth, and root water potential measured midday (mm)
RAW_{low}	Readily available water content in the root zone in low ECa regions (mm)
RAW_{mid}	Readily available water content in the root zone in depth in mid ECa regions (mm)

RAW_{high}	Readily available water content in the root zone in high ECa regions (mm)
REW	Cumulative depth of evaporation (mm)
RH	Mean daily relative humidity (%)
R_n	Solar radiation ($W\ m^{-2}$)
RO_i	Run off at the end of day i (mm)
S	Slope of the saturation vapour pressure ($kPa/^\circ C$)
T_m	Mean temperature ($^\circ C$)
T_{max}	Max temperature ($^\circ C$)
T_{min}	Min temperature ($^\circ C$)
TAW_{RF}	Total available water in the root zone (mm) adjusted to soil texture
TAW_{RD}	Total available water in the root zone (mm) adjusted to soil texture and variable root depth measured
TAW_{Ψ}	Total available water in the root zone (mm) adjusted to soil texture, variable root depth, and root water potential measured midday
$TEW_{RF,RD}$	Maximum evaporable water defined according the soil texture analyses
TEW_{Ψ}	The maximum evaporable water, which defined according the soil texture analyses and the midday root water potential as wilting point
u	Wind speed ($m\ s^{-1}$)
WB	Water balance model (mm)
WB_{RF}	Water balance model (mm) soil-adjusted
WB_{RD}	Water balance model (mm) adjusted to soil and rooting depth
WB_{Ψ}	Water balance model (mm) adjusted to soil, rooting depth and midday root water potential
WP	Wilting point, index 0 ranging from -1.50 to -1.01 MPa, while Ψ refers to root water potential measured midday
Z_c	Effective depth of soil evaporation layer (m)
Z_R	Root depth measured (m)
Z_0	Uniform root depth of 1 m (Allen et al. 1998) for apple trees
γ	Psychrometric coefficient ($kPa/^\circ C$)
ρ	Apparent soil resistivity ($\Omega\ m$)
Θ_{FC}	Volumetric soil water content at field capacity (FC) ($m^3\ m^{-3}$)
Θ_{WP}	Volumetric soil water content at WP_0 ($m^3\ m^{-3}$)
Θ_{Ψ}	Volumetric soil water content at wilting point ($m^3\ m^{-3}$) according to root water potential measured midday

Introduction

In the fruit production, the variability of growth factors, under or overrunning the plant needs, has to be regarded as a reason for the waste of resources or loss of yield. The use of new technologies in agriculture has facilitated the measurement of spatial and temporal variability of yield parameters and field properties (Sudduth 1999). The concept of precision agriculture (Auernhammer 2001; Blackmore et al. 2003) serves as a driver for the progress in the development of sensor applications, the communication and geographical information systems (GIS), and variable rate application in order to reflect the spatial and temporal variability. The use of similar approaches in fruit production has been discussed (Zude-Sasse et al. 2016; Pathak et al. 2019), but research has not explored the full potential of increasing the spatially resolution in fruit production management.

In orchards, the spatial variability of soils is a major factor influencing the need for irrigation water and fertilizer. In apple, pear, plum, and citrus orchards, high variability of soil texture has been reported frequently (Naor et al. 2006; Käthner et al. 2017). Despite the variety of soil sensors available, electrical sensors have been most often utilized in orchards for spatial soil characterization. Electrical conductivity (EC) and apparent electrical conductivity (ECa) of soil are affected by a number of parameters such as salinity, soil texture, humidity, roots, and other organic matter (Corwin and Plant 2005; Humphreys et al. 2005; Shaner et al. 2008). Thus, ECa measurement provides valuable information for the patterns of soil properties in the field and can allow the delineation of zones.

Consequently, if laboratory reference data of the soil are available, the spatial variability of the soil can be derived by the ECa measurement even if many potentially perturbing factors need to be considered. A methodology for guided soil sampling using ECa data was suggested (Horney et al. 2005) for targeting samples of each ECa zone. The steps are to map ECa, delineate zones, and identify the locations for soil sampling (Shaner et al. 2008). This method has been successfully applied in fields, orchards, and vineyards (Daccache et al. 2014; Hedley and Yule 2009; Oldoni and Bassoi 2016). Also, ECa mapping has been frequently used for guided soil sampling and the mapping of available water content by means of clustering algorithms (Haghverdi et al. 2015; Peeters et al. 2015). However, when measuring at field capacity, then the ECa is assumed to be influenced mainly by soil texture and soil water content. This is exactly interesting considering the plant water supply.

Hedley and Yule (2009), reported that the spatial variation in soil water retention characteristics was strongly correlated with the spatial variation in soil texture across a field, noting that obviously areas with heavier soil zones within a field had an increased water-holding capacity in comparison to those with light textured soils showing increased percentage of enhanced particle size related to sand. Therefore, when calculating the water balance of an orchard, the texture determines the field capacity which is crucial for calculating the total available water content of the soil (TAW). So, ECa maps might be used for precision irrigation if they mainly represent the TAW. An example of variable rate irrigation based on ECa maps and TAW was shown earlier (Hedley et al. 2010).

Besides soil parameters determining the water supply, water consumption is affected by plant properties, such as the rootstock (Tworkoski et al. 2016), developmental stage (Allen et al. 1998), crop load (Haberle and Svoboda 2015; Hunsaker et al. 2015), and plant response to drought stress such as the change in solute content per cell (osmotic adjustment) (Dodd et al. 2010; Lauri et al. 2013). Thus, plant parameters need to be considered during the calculation of TAW (Allen et al. 1998; Haberle and Svoboda 2015; Hunsaker et al. 2015). A water balance model based on observed and calculated TAW considering the root depth and water depletion was developed for several annual crops, such as potatoes, maize, cereals, sugar beet, and oil seed rape (Haberle and Svoboda 2015) in temperate climate. When calculating the TAW in orchards, particularly in the perennial fruit trees, the root depth should be considered, since the effects of soil texture and available water on root growth accumulate (Levin et al. 1979; Phogat et al. 2013; Pérez-Pastor et al. 2014).

Furthermore, trees may respond to short-term changes of TAW in the root zone: In drought stress situations, the root water potential may be affected by means of physiological mechanisms such as decreased osmotic potential (Herppich and Geyer 2001; Blum 2017). Such decrease would lead to reduced root water potential (ψ) and resulting enhanced capability of the root to obtain water from the soil. By definition, the root water potential represents the actual wilting point accounted in the calculation of readily available water content (RAW). Both, TAW and RAW are calculated considering the field capacity and wilting point.

TAW and RAW are used for analyzing the actual evapotranspiration (ET_a) aimed at calculating the water balance of an orchard. The methods that are used for the estimation of ET_a , are either empirical (Courault et al. 2005) or climate data driven (Verstraeten et al. 2008). The last category utilizes meteorological data from weather stations. The Penman–Monteith method is commonly used to calculate the ET_a (Allen et al. 1998; Jensen et al. 1990). For orchard management, only water balance methods can provide the required level of detail (Alexandridis et al. 2014; Hunink et al. 2015). However, the water balance at an even finer spatial scale might become desirable, when the soil shows spatial variability and response of trees to the growth factors can be demonstrated.

The general hypothesis was that water needs in an apple orchard can vary over space and time. Further, it was hypothesized that this spatial variation is governed by spatial patterns of soil water holding capacity and the crop's adaption to the soil properties. Specific knowledge gaining addressed (i) how three different levels of information on RAW (spatially uniform reference root depth (RAW_{RF}), actual measured root depth (RAW_{RD}), and root water potential (RAW_{ψ})) affect RAW irrigation thresholds, and (ii) how estimation of water needs is affected by spatially resolved daily water balance according to zones of low, medium, and high ECa values considering the three cases of RAW.

Materials and methods

Site description

The experiment was conducted in a commercial apple orchard (6 ha), Brandenburg, Germany, during 2017. The orchard was planted with 4×1 m distance of *Malus × domestica* 'Gala', budded onto dwarfing M9 rootstock. Apple trees were trained as slender spindles with a central leader branch pruned to maximum height of 2.8 m. Ground cover in the rows was removed throughout the season. Drip irrigation was carried out field-uniform throughout the vegetation period. Despite a slight gradual slope of about 4° , the water pressure was similar in all locations. The northern part had visually poorer soil properties compared to the southern part where the soil was deeper, and visually appeared more fertile (Fig. 1).

The soil ECa measurement was conducted using galvanic coupled resistivity system with a Wenner electrode configuration at field capacity. The four electrodes were equidistantly spaced in a straight line at the soil surface, with the two outer electrodes serving as the current or transmitters electrodes, while the two inner electrodes serving as the potential or receivers electrodes. The depth of investigation (DOI) is defined by the inter-electrode spacing. It was set to 50 cm, which corresponds to a DOI of 25 cm. The measurements provided soil resistivity (Eq. 1), which were converted to ECa (Eq. 2).

$$\rho = 2\pi m(\Delta V/I) = 2\pi m R \quad (1)$$

$$ECa = 1/\rho \quad (2)$$

where ρ represented the soil resistivity (Ω m), m the electrode spacing (m), ΔV the difference of voltage (V), I the current (A) and R the resistance (Ω). The reciprocal of ρ was utilized in order to calculate the ECa (mS/m). The data were obtained for every third tree

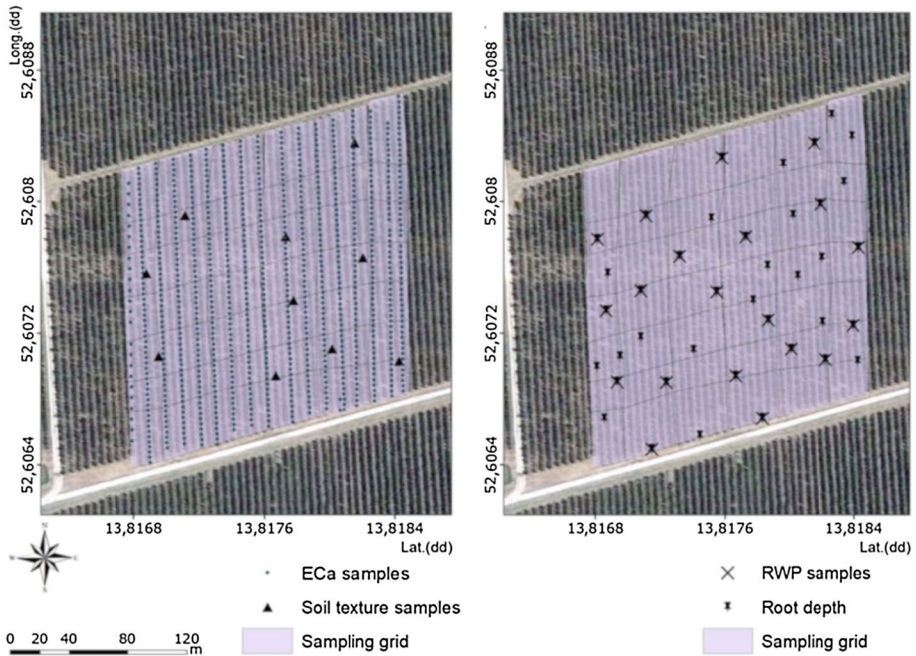


Fig. 1 Site description of the apple orchard showing the sampling grid: The sampling locations are depicted for apparent soil electrical conductivity (ECa) and soil texture (left), rooting depth and root water potential (RWP) (right)

and every second row ($n=563$), the values were saved from the data logger (4-Point Light, LGM, Schauffling, Germany) and analyzed in ArcGIS (10.2.2 ESRI, USA).

Guided soil sampling

After calculating the ECa map, 10 sampling locations covering the range of ECa values within the orchard were selected. Samples were collected in 30 cm and 60 cm depth using an Edelman combined soil sampler. The samples were analyzed with sedimentation method that is based on difference in settling time of particles having different sizes defined as clay, silt, and sand from which the soil texture is constructed (Taubner et al. 2009). In parallel with soil sampling, the root depth was measured for each tree of soil analysis plus 40 trees, according to the ECa variation ($n=50$). The soil around the root was rinsed out with water and the root depth was determined as the end of roots visible with this method. Since the method is partly destructive, trees were excluded from yield monitoring. On 75 additional soil samples, cores were retrieved in 30 cm and 60 cm and subjected to oven-drying for 2 days at 105 °C in order to analyze bulk density and porosity.

Root water potential

The roots were sampled with soil core samplers and a knife at 10–20 cm depth for each sample tree. A Scholander pressure chamber (Plant Water Status Console 3000, Soil moisture

Equipment Corp., USA) was utilized for measuring the root water potential (ψ). The root was sealed in the chamber. When the pressure was enhanced in the chamber, the pressure reached and extended the pressure of the root and, as a result, the cells of the xylem leaked water (Turner 1988). At the equilibrium point, when the pressure in the chamber equals the pressure of the root water potential (MPa), the pressure was recorded (Herppich and Geyer 2001).

The measurement was carried out during full bloom, cell division, and harvest. An average out of four measurements was taken for each individual tree sampled ($n = 20$). The minimum root water potential (Ψ_{midday}) and maximum values (Ψ_{dawn}) were measured during midday and dawn, respectively. The midday value was assumed to be equal to the actual wilting point (WP_{ψ}). Subsequently, the Van Genuchten model was utilized for calculation of volumetric water content at WP_{ψ} considering sandy loamy soil (Carsel and Parrish 1988; van Genuchten and Pachepsky 2011).

Water balance

Evapotranspiration

The meteorological data were recorded by the weather station (IMT 280, Pessl, Austria) located inside the field. The station recorded air temperature (T), relative humidity (RH), wind speed (u), solar radiation (R_n) and stored in the database <http://technologygarden.atb-potsdam.de>. For calculating the water balance according to Penman–Monteith, the reference evapotranspiration (ET_0) (Eq. 3) provided the reference for the actual evapotranspiration (ET_a), as proposed in FAO-56.

$$ET_0 = \frac{0.408s(R_n - G) + \gamma \frac{900}{T_m + 273} u(e_s - e_a)}{s + \gamma(1 + 0.34u)}, \quad (3)$$

with the daily net radiation at the surface [R_n (MJ/m² day)], soil heat flux [G (MJ/m² day)], which was assumed to be zero on the daily scale (Allen et al. 1998), and daily average air temperature [T_m (°C)] (Eq. 4)

$$T_m = (T_{\text{max}} + T_{\text{min}})/2, \quad (4)$$

with T_{max} and T_{min} representing the maximum and minimum daily air temperatures, respectively, the average wind speed at 2 m above the surface [u (m/s)]; the saturation vapour pressure [e_s (kPa)] and the actual vapour pressure [e_a (kPa)]. The γ represented the psychrometric coefficient (kPa/°C) and s (kPa/°C) was the slope of the saturation vapour pressure at T_m . The estimates of the net radiation and the aerodynamic terms were based on the FAO-56 paper (Allen et al. 1998).

The three cases of crop evapotranspiration (ET_a) tested in the present study (Eqs. 5–7) were obtained by (i) multiplying the ET_a (mm/day) with the soil water stress co-efficient (K_s) and adding the soil surface evaporation coefficient (K_e), using one ET_a (Allen et al. 2005) for the entire orchard as well as (ii) implementing the spatial information on root depth ($ET_{a,RD}$), and (iii) root water potential data ($ET_{a,\psi}$) as shown subsequently.

$$ET_{a,RF} = (K_{s,RF}K_{cb} + K_{e,RF,RD}) ET_0 \quad (5)$$

$$ET_{a,RD} = (K_{s,RD}K_{cb} + K_{e,RF,RD}) ET_0 \quad (6)$$

$$ET_{a,\psi} = (K_{s,\psi}K_{cb} + K_{e,\psi}) ET_0 \quad (7)$$

The K_{cb} coefficient was in all cases calculated for three phenological stages: The value for the initial-season ($K_{cb,ini}$) from the bud break till the full bloom was set at 0.8 (Allen et al. 1998; Table 12), while for mid-season ($K_{cb,mid}$) from full bloom till the harvest period and for end-season ($K_{cb,end}$) from the harvest period till defoliation the values were calculated (Eqs. 8, 9).

$$K_{cb,mid} = K_{c,mid(tab)} + [0.04(u - 2) - 0.004(RH_{min} - 45)] \left(\frac{h}{3}\right)^{0.3} \tag{8}$$

$$K_{cb,end} = K_{c,end(tab)} + [0.04(u - 2) - 0.004(RH_{min} - 45)] \left(\frac{h}{3}\right)^{0.3} \tag{9}$$

where $K_{c(tab)}$ were set at $K_{c,mid(tab)}=1.20$ and $K_{c,end(tab)}=0.85$ as commonly used (Allen et al. 1998; Table 12). The RH_{min} was the mean daily minimum relative humidity (%) for the initial-season, mid-season, end-season, and h was the mean crop height of 3 ± 0.5 m. The duration of the phenological stages for Gala apple tree was set for a deciduous orchard of low altitude; the initial period lasted 23 days after bud break, mid-season 190 days, and end season 60 days (Allen et al. 1998).

RAW irrigation thresholds

The soil water stress coefficient (K_s) used in Eqs. 5–7, and the total (TAW) and readily available soil water content (RAW) for high depletion of water from the root zone (D_r), with $D_r > RAW$ (Pereira et al. 2015) were calculated according to Eqs. 10–12:

$$K_{s,RF} = \frac{TAW_{RF} - D_r}{TAW_{RF} - RAW_{RF}} \tag{10}$$

$$K_{s,RD} = \frac{TAW_{RD} - D_r}{TAW_{RD} - RAW_{RD}} \tag{11}$$

$$K_{s,\Psi} = \frac{TAW_{\Psi} - D_r}{TAW_{\Psi} - RAW_{\Psi}} \tag{12}$$

with

$$D_{r,i} = D_{r,i-1} - (P_i - RO) - I_i + ET_{a,i} + DP_i \tag{13}$$

$$DP_i = P_i + I_i - ET_{a,i} - D_{r,i-1} \tag{14}$$

Variables used captured the depletion of the water in the root zone $D_{r,i}$ expressed daily by an estimation (mm) (Eq. 13), the water content in the root zone at the end of the previous day [$D_{r,i-1}$ (mm)], the precipitation on day i [P_i (mm)], the runoff from the soil surface on day i [RO_i (mm)] assumed zero, the net irrigation depth on day i that infiltrates the soil [I_i (mm)]. The irrigation events took place early in the morning, with 6 mm per day regardless the actual weather conditions. DP_i (mm) was the water loss out of the root zone by deep percolation on day i calculated only during high precipitation (Eq. 14). The $D_{r,i}$ (Eq. 13) was recorded for each of the sampling points according to guided sampling derived from soil ECa, considering Eca_{low} , Eca_{mid} , Eca_{high} .

and with

$$TAW_{RF} = 1000(\Theta_{FC} - \Theta_{WP})z_0 \quad (15)$$

$$TAW_{RD} = 1000(\Theta_{FC} - \Theta_{WP})z_{RD} \quad (16)$$

$$TAW_{\psi} = 1000(\Theta_{FC} - \Theta_{\psi})z_{RD} \quad (17)$$

TAW_{RF} (mm) was the total available soil water for the root zone assuming field-homogeneous root depth of 1 m and WP of -1.5 MPa. TAW_{RD} was considering the measured root depth and WP at -1.5 MPa, while TAW_{ψ} was taking into account the measured root depth and the midday root water potential as WP.

The volumetric water content at field capacity [Θ_{FC} (cm^3/cm^3)] was set according to the German soil classes (Sponagel et al. 2005) based on the soil particle size distribution measured. The Θ_{WP} was either the volumetric water content (cm^3/cm^3) at wilting point (WP) that was assumed -1.5 MPa or Θ_{ψ} calculated according to the midday Ψ (MPa), z_0 is the average root depth for the apple trees as indicated by FAO with 1 m, while z_{RD} was the measured rooting depth (m) (Eqs. 15–17).

and with

$$RAW_{RF} = p TAW_{RF} \quad (18)$$

$$RAW_{RD} = p TAW_{RD} \quad (19)$$

$$RAW_{\psi} = p TAW_{\psi} \quad (20)$$

with

$$p = p_{\text{tab}} + 0.04(5 - ET_a) \quad (21)$$

The RAW (mm) (Eqs. 18–20) represented thresholds for water stress. It was estimated on daily basis according to the soil texture analyses. Consequently, three thresholds were considered in the spatial water balance as shown below. Where RAW_{RF} and RAW_{RD} referred to rooting depth of 1 m and measured root depth, respectively. RAW_{ψ} being the readily available soil water content measured by means of root water potential during full bloom, fruit cell division stage, and harvest. The average fraction of TAW that can be depleted from the root zone before the revealing of moisture stress was p (Eq. 21), where p_{tab} equaled a constant value as recommended by Allen and co-workers (Allen et al. 1998), while ET_a was calculated according to the three cases as shown above (Eqs. 5–7).

Soil evaporation

For considering the assumed spatial variability of soil texture and evaporation in the water balance model, the K_e for the mid or the last growth stage was calculated according to previous experiments (Allen et al. 1998; Paço et al. 2012) (Eqs. 22, 23), where the maximum value of K_{cb} during the cultivation period ($K_{cb,\text{max}}$) was implemented. The estimation of K_e took place when the soil started to dry. In other words, when the daily cumulative depth of water depleted from the surface ($D_{e,i}$) exceeded the readily evaporable water (REW, see below). This can be defined by the soil evaporation reduction coefficient (K_r) (Eqs. 24, 25). The REW was 8 mm for loamy sand and 10 mm for sandy loam region (Allen et al. 1998; Table 12). $TEW_{RF,RD}$ (Eq. 26) was the maximum evaporable water defined according to

the soil texture analyses, whereas in TEW_{Ψ} (Eq. 27) the values of root water potential were considered as WP. Furthermore, Z_e is the depth of soil that can be dried from evaporation, which was 12 mm for loamy sand region and 16 mm for sandy loam region (Allen et al. 1998; Table 12).

$$K_{e,RF,RD} = K_{r,RF,RD}(K_{cb,max} - K_{cb,mid,end}) \tag{22}$$

$$K_{e,\Psi} = K_{r,\Psi}(K_{cb,max} - K_{cb,mid,end}) \tag{23}$$

$$K_{r,RF,RD} = \frac{TEW_{RF,RD} - De_i}{TEW_{RF,RD} - REW} \tag{24}$$

$$K_{r,\Psi} = \frac{TEW_{\Psi} - De_i}{TEW_{\Psi} - REW} \tag{25}$$

with

$$TEW_{RF,RD} = 1000(\Theta_{FC} - 0.5\Theta_{WP}) Z_e \tag{26}$$

$$TEW_{\Psi} = 1000(\Theta_{FC} - 0.5\Theta_{\Psi}) Z_e \tag{27}$$

Furthermore, the cumulative depth of evaporation at the end of the previous day [$D_{e,i-1}$ (mm)], daily evaporation [$E_{a,i}$ (mm)] were considered. The fraction of wetted soil surface (f_w) as well as the exposed and wetted soil fraction f_{ew} were calculated according to previous experiments (cf. Allen et al. 1998). $DP_{e,i}$ was considered when the Z_0 exceeded the field capacity. The $D_{e,i}$ (Eq. 28) was calculated for each of the sampling points according to guided sampling derived from soil ECA, considering ECA_{low} , ECA_{mid} , ECA_{high} .

$$D_{e,i} = D_{e,i-1} - (P_i - RO) - I_i f_w^{-1} + E_i f_{ew}^{-1} + DP_{e,i} \tag{28}$$

$$DP_{e,i} = P_i + I_i f_w^{-1} D_{e,i-1} \tag{29}$$

Water needs

The three different ET_a cases were implemented in the water balance (WB) of the orchard, field-homogeneously and considering the spatial variability of plant data. It should be noted that for each case $K_{s,RF}$, $K_{s,RD}$ and $K_{s,\Psi}$, necessary for ET_a analysis (see above), were calculated according to the measured soil texture from soil samples using the values indicated for soil texture in Germany, while only $K_{s,RF}$ was calculated without taking into account the plant response (Sponagel et al. 2005). Thus, the three water balance models (Eqs. 22–24) derived (mm/day) are described by the following equations, where P is the daily precipitation (mm):

$$WB_{RF} = ET_{a,RF} - P \tag{30}$$

$$WB_{RD} = ET_{a,RD} - P \tag{31}$$

$$WB_{\Psi} = ET_{a,\Psi} - P \tag{32}$$

Data analysis

In this study, ECa sampling grid was the largest grid with 42 cells (10 X 20 m), consequently it was used as the reference grid. A GIS software package (ArcGIS, ESRI, Inc., USA) was utilized to calculate the mean values for the measured parameters in each of the 42-grid cell. Initially the grid layer was formed as polygons. The measured parameters, initially given as point data, were joined with the grid layer by averaging the values of the points that fall in the each grid cells. Hence, the samples were categorized and compared according to the ECa zones: low, mid and high.

Outliers due to gaps that were created by missing trees in the field were removed from the dataset. The maps give a general view for each measurement and enable the control of values that produce error. For mapping, ordinary Kriging method was used to interpolate the ECa and the root depth data according to the variograms (Panagopoulos et al. 2006). Thus, least squares regression was utilized with a spherical model semivariogram for ECa and root depth based on leave one out cross validation. To avoid overlaps, the number of neighbors (lag) in variograms was defined with the averaged nearest neighbor method that computes the average distance between points and their nearest neighbor. Spherical and a stable variogram models were fitted for the ECa and the root depth to interpolate maps by ordinary Kriging. Data were separated in three groups with the same number of values. The analysis was carried out in ArcGIS (Version 10.2.2, ESRI, USA).

Non-spatial data analysis was carried out for data collected at the ECa using Matlab (Version R2017a, Mathworks Inc., Natick, MA, USA). These include descriptive statistics for mean value, range and standard deviation. The dependency of ECa on soil texture was assessed by analysis of variance (ANOVA), while Pearson's r coefficient of correlation was calculated to quantify the linear relationships among the variables. Due to the presence of spatial autocorrelation the correlation might be overoptimistic and no p values were presented for ECa and plant data. A Friedman and Corwin analysis was done for the comparison of the three water balance models that have been estimated for each individual ECa zone.

Results and discussion

Soil texture and ECa considering guided sampling

Samples acquired at 30 cm showed enhanced variation (Table 1) compared to samples taken at 60 cm. The soil was mainly composed of sand and more specifically with fine sand in both depths. However, the bulk density showed a higher coefficient of variance at 60 cm ($CV = 21.88\%$) than in 30 cm ($CV = 12.43\%$). In general, the soil is characterized as loamy sand and silty sand, with the enhanced quantities of fine sand, medium sand and coarse sand. The field had a slope heading to the south and, consequently, soil particles from the elevated part would probably migrate towards the lower part of the field.

The results from ANOVA considering ECa as dependent factor of the soil classes showed that ECa was affected by the sandy soils. More specifically, the ECa appeared influenced by medium silt, with $F = 3.91$ and also ECa was influenced by medium sand with $F = 7.55$. However, no further relationship was observed between ECa and remaining soil classes. Silt was positively related with ECa, while sand illustrated a negative correlation (Table 2). Furthermore, bulk density correlated positively with sand and medium

Table 1 Descriptive statistics for particle size distribution, bulk density, and volumetric water content at field capacity (FC_0) and wilting point (WP_0) in 30 cm, as well as apparent electrical conductivity (ECa) providing standard deviation (SD), coefficient of variance (CV), ($N=10$)

	Range	Minimum	Maximum	Mean	SD	Variance	CV %
Fine silt ($mg\ kg^{-1}$)	2.60	1.80	4.40	3.07	0.93	0.87	30.36
Medium silt ($mg\ kg^{-1}$)	3.60	3.50	7.10	6.00	1.26	1.60	21.08
Coarse silt ($mg\ kg^{-1}$)	2.50	13.30	15.80	14.41	0.96	0.93	6.68
Fine sand ($mg\ kg^{-1}$)	2.10	34.50	36.60	35.23	0.73	0.54	2.086
Medium sand ($mg\ kg^{-1}$)	5.10	27.10	32.20	29.81	1.65	2.71	5.51
Coarse sand ($mg\ kg^{-1}$)	2.10	4.30	6.40	5.55	0.61	0.37	10.91
Bulk density ($g\ cm^{-3}$)	0.45	0.74	1.19	1.01	0.13	0.02	12.43
ECa (mS/m)	74.76	11.95	86.70	46.90	14.29	1.06	30.46
Root depth (cm)	24.00	17.00	26.00	20.50	2.38	0.87	11.60
FC_0 (cm^3/cm^3)	6.00	23.00	29.00	25.80	2.09	4.38	8.11
WP_0 (cm^3/cm^3)	5.00	4.00	9.00	6.90	1.37	1.88	19.89

sand. Similar results were obtained earlier by Corwin and Lesch 2013, concluding that the ECa is influenced by the soil texture and the soil moisture (Hedley and Yule 2009; Suduth et al. 2005). A significant negative correlation was found between ECa and root depth ($r=-0.822$). Moreover, sand, medium sand, and coarse sand depicted a positive correlation with the root depth, while root depth was negatively correlated with silt.

Spatial patterns of ECa and rooting depth

The values of ECa varied between 2.99 and 11.71 $mS\ m^{-1}$. The rooting depth measured was approximately at 20 cm, with C.V. = 18.82%, whereas FAO suggests a minimum root depth of 1 m for apple trees. The shallower root system appeared mostly in the south and in the center north part of the field, whilst roots were deeper in the south west and south east part. Enhanced values of ECa were measured in the south part and in the middle north part of the field, while in the west and the east part lower values were measured (Fig. 2). A high negative relationship was observed between the ECa and the root depth with $r=-0.80$ and $r=-0.58$ in low and high ECa regions, respectively.

The correlation can be explained by the main effects of penetration resistance and water supply. In the present study, the mean value of bulk density was 1.00 $g\ cm^{-3}$ at 30 cm and 1.08 at 60 cm, which represents a range that provides no extreme growing conditions allowing normal root development (Dodd et al. 2010; Ferree and Streeter 2004). However, it was assumed that the soil texture affected the depth of the root. Estimation of the root depth from the ECa has been approached earlier in vines (Rodríguez-Pérez et al. 2011; Trought and Bramley 2011). Consistently, in a study on rootstocks of Starkspur Supreme Delicious in sandy loam soils, the root reached deeper soil layers compared to soil with smaller particle size (Fernandez et al. 1995). Furthermore, the water holding capacity decreases in sandy areas showing low ECa. McCutcheon et al. 2006 suggested that the spatial variability of ECa is a good indicator for predicting soil water content. ECa measurement was already proposed for a variable rate application of water in many studies (Hedley and Yule 2009, Lo et al. 2017). The relationship of elevation, ECa measured in dry conditions, and growth of fruit trees was compared recently (Käthner et al. 2017). In an

Table 2 Pearson correlation among soil classes, apparent electrical conductivity (ECa), bulk density and root depth

	ECa (mS m ⁻¹)	Root depth (cm)	Bulk density (g m ⁻³)	Fine silt (mg kg ⁻¹)	Medium silt (mg kg ⁻¹)	Coarse silt (mg kg ⁻¹)	Fine sand (mg kg ⁻¹)	Medium sand (mg kg ⁻¹)	Coarse sand (mg kg ⁻¹)
ECa (mS m ⁻¹)	1	-0.739**	-0.163	0.076	0.467**	0.116	-0.027	-0.436*	-0.348
Root depth (cm)		1	-0.112	-0.155	-0.287	-0.239	0.316	0.564**	0.486*
Bulk density (g m ⁻³)			1	0.004	-0.102	-0.297	-0.051	0.562**	0.358

Correlation was significant at 0.01 (**), 0.05 (*) level

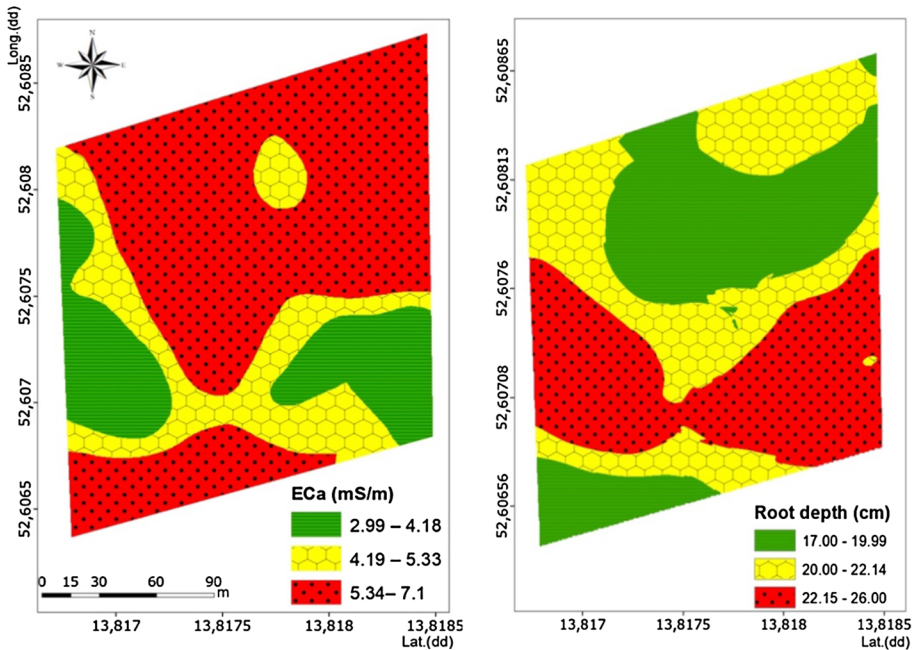


Fig. 2 False color maps of apparent electrical conductivity, ECa (mS m^{-1}) of soil in 1 m (left) and predicted root depth (cm) (right)

experiment on the ECa estimation, in which the soil was at field capacity and in non-saline conditions, the spatial variability of TAW was described more precisely by a contact and electrode based sensor in shallow root depth ($R^2=0.77$) (Hezarjaribi and Sourell 2007). Taking the sum of influences of penetration resistance and available water content on the root depth into account, the negative correlation of soil ECa and rooting depth appears reasonable. This remains true, even if the effect may be compromised by enhanced root density close to the drip irrigation (Watson et al. 2006). However, drip irrigation was uniform in the entire orchard.

Thus, a 10×20 m grid was created for the ECa and the root depth. In the variogram of root depth a nugget effect around 0.1 was observed. On the contrary no nugget effect was found in the variogram for ECa. The lag in both variograms was reached approximately at 5 m, with a sill around 1 for the ECa ($\sim 1 \text{ mS/m}$) and 0.8 ($\sim 0.89 \text{ cm}$) for the root depth (Fig. 3). According to Cambardella et al. (1994), the nugget to sill ratio lower than 25% indicates strong spatial dependence; between 25 and 75% denotes moderate spatial dependence and greater than 75% indicates weak spatial dependence. In this experiment, the ratio was 12.5% for the root depth indicating a strong spatial dependence. The ECa with zero nugget effect confirmed a strong spatial dependence. This was an additional support to consider kriging as the optimum interpolation method (Moral et al. 2011), while p values were avoided due to assumable overestimation.

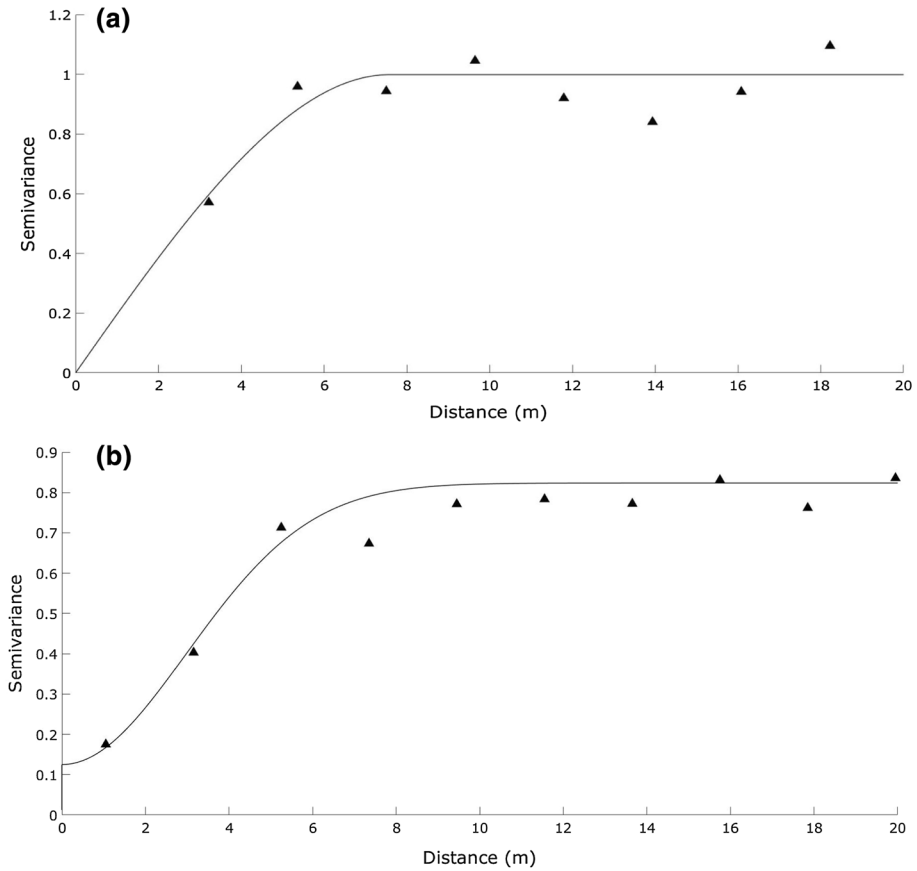


Fig. 3 Fitted semivariogram models for apparent electrical conductivity of soil, ECa (a) and for rooting depth (b)

Total available soil water content (TAW) considering rooting depth and root water potential

According to Green et al. (2003), the water uptake in mature apple trees is based mainly from the shallow, dense root system, but also uses deeper roots. In the present study, TAW was calculated for the root depth assuming 1 m and the actual root depth obtained by regression from ECa data. The TAW_{RF} point to increased water contents compared to the TAW_{RD} that corresponds to the shallower root system found for the dwarfing rootstock M9. This rootstock is widely used in the apple production world-wide and the enhanced water needs should be considered when constructing the irrigation system in practice. The patterns of TAW_{RF} and TAW_{RD} appeared similar, showing areas with increased water content mainly in the center and the north of the field (Fig. 4). An area with low TAW crosses the field, with the majority to be observed in the south region of the field. However, the actual rooting depth allows water uptake in reduced soil volume and, consequently, TAW_{RD} appeared reduced. As it can be assumed, a positive correlation was depicted between the root depth and the TAW_{RD} considering separately low ECa regions ($r=0.68$) and high ECa

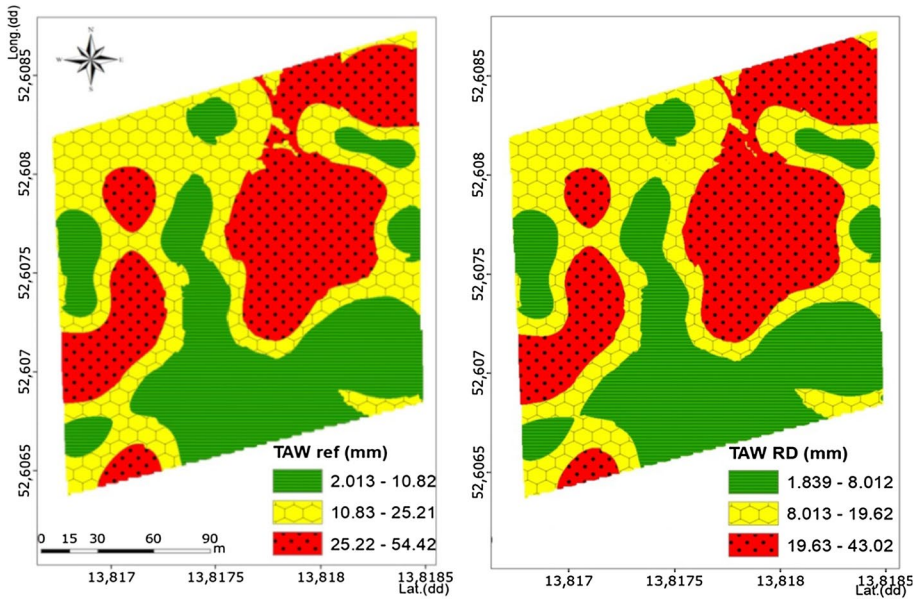


Fig. 4 False color map of total available water content (TAW_{RF}) for field-homogeneous root depth at 1 m (left), and TAW_{RD} considering measured root depth (right). The red color and dots depict the regions with high water content in the root zone, whilst the green areas indicate regions with low water content

Table 3 Pearson correlation among soil classes, apparent electrical conductivity (ECa), rooting depth, total available water content for assumed root depth of 1 m (TAW_{RF}) and total available water content for measured root depth (TAW_{RD})

	ECa (mS m ⁻¹)	Root (cm)	TAW_{RD} (mm)	TAW_{RF} (mm)
Low ECa				
ECa	1			
Root	-0.80**	1		
TAW_{RD}	0.75*	-0.29	1	
TAW_{RF}	0.39	0.08	0.68*	1
Mid ECa				
ECa	1			
Root	-0.37	1		
TAW_{RD}	0.50*	0.17	1	
TAW_{RF}	0.26	0.34	0.89*	1
High ECa				
ECa	1			
Root	-0.58**	1		
TAW_{RD}	0.47*	-0.41	1	
TAW_{RF}	0.37	-0.36	0.19	1

Correlation is significant at 0.01 level (**) and at 0.05 (*)

($r=0.89$). Furthermore, correlation was found of ECa and TAW_{RD} in low ($r=0.75$), in mid ($r=0.50$) and in high ($r=0.47$) ECa regions (Table 3). The regions with deeper root system had an enhanced amount of TAW_{RD} and vice versa for the shallower root systems (Fig. 4).

Table 4 Descriptive statistics for root water potential (Ψ ; MPa) measured (N=20) midday and dawn in full bloom ($\Psi_{F, \text{midday}}$, $\Psi_{F, \text{dawn}}$), in cell division phase ($\Psi_{C, \text{midday}}$, $\Psi_{C, \text{dawn}}$), and at harvest ($\Psi_{H, \text{midday}}$, $\Psi_{H, \text{dawn}}$); the soil water potential at field capacity (FC) and assumed wilting point (WP_0) considering the soil texture and corresponding volumetric water content (VWC; cm^3/cm^3)

	Low ECa		Mid ECa		High ECa	
	Mean \pm SD	VWC	Mean \pm SD	VWC	Mean \pm SD	VWC
$\Psi_{F, \text{midday}}$	-1.48 ± 0.77	6.57	-1.3 ± 0.35	6.76	-1.6 ± 1.01	6.78
$\Psi_{F, \text{dawn}}$	-0.71 ± 1.02	5.82	-0.98 ± 0.30	5.78	-1.24 ± 0.85	5.79
$\Psi_{C, \text{midday}}$	-1.33 ± 0.53	5.75	-1.25 ± 0.45	5.76	-1.59 ± 0.97	5.76
$\Psi_{C, \text{dawn}}$	-0.66 ± 0.88	5.83	-0.68 ± 0.17	5.83	-0.77 ± 0.67	5.85
$\Psi_{H, \text{midday}}$	-1.18 ± 0.77	5.76	-1.05 ± 0.35	5.77	-1.51 ± 1.01	5.77
$\Psi_{H, \text{dawn}}$	-0.63 ± 0.62	5.84	-0.74 ± 0.38	5.82	-0.89 ± 0.71	5.83
FC	-0.33	22.3	-0.3	25	-0.26	27
WP_0	-1.5	6.00	-1.2	7.00	-1.01	8.00

The root water potential related positively during dawn and midday, which signifies that the trees suffered no severe drought stress as indicated by resaturated tissue in the morning, and values decreasing during midday due to the open stomata and active photosynthetic apparatus. The root water potential varied between -0.6 MPa measured dawn and -1.6 MPa measured midday. The values are in the range measured earlier (Dodd et al. 2010; Whitmore and Whalley 2009). The root water potential measured midday was utilized further to address the most crucial water deficit situation, considering many earlier studies (Naor et al. 1999). The root water potential midday defined the actual wilting point (WP) and, therefore, the volumetric soil water content accessible by the tree. This plant-specific approach was utilized when calculating TAW_{Ψ} .

For the generally assumed $WP_0 = -1.5$ MPa and the soil texture measured in low ECa region, the volumetric water content equaled $6 \text{ cm}^3/\text{cm}^3$. When considering the variability of soil texture, the volumetric water content at WP_0 was enhanced till $8 \text{ cm}^3/\text{cm}^3$ (Table 4). The actual wilting point of the trees midday, varied marginally in the phenological stages of the tree. The volumetric water content of the soil, calculated according to van Genuchten (van Genuchten and Pachepsky 2011), appeared in the range of the assumed WP_0 . It should be mentioned that the C.V. % among the Ψ values measured at dawn did not vary vastly with C.V._F = -21.2% , C.V._C = -17.57% and C.V._H = -16.57% .

ECa showed a positive correlation with $\Psi_{F, \text{dawn}}$ and $\Psi_{H, \text{dawn}}$ ($r=0.463$ and $r=0.678$). Another considerable positive correlation occurred between bulk density and the root water potential midday during cell division and during harvest ($r=0.478$ and $r=0.567$). However, it may be concluded that the fruit trees showed no ability to adapt to the variation in water supply by means of osmotic adjustment in the present study. Consistently, the $TAW_{F, \Psi}$, $TAW_{C, \Psi}$ and $TAW_{H, \Psi}$ showed that the coefficient of variation point to no difference with C.V. = 16.23% , C.V. = 17.84% , C.V. = 13.60% and C.V. = 14.36% , respectively. However, it is well noted that the root water potential is affected by many factors such as rootstock (Tombesi et al. 2009) and abscisic acid (Hurley and Rowarth 1999; Puértolas et al. 2014) and, therefore, results may differ in other situations.

RAW irrigation threshold

According to the daily weather data, the highest temperatures were observed during June and July (Fig. 5). Between May and August the highest precipitations, above 40 mm, have been monitored. 2017 was extremely wet with precipitation of 724 mm year⁻¹ compared to the average annual precipitation over 30 years of 585 mm in this fruit production region. During bud break and full bloom small but frequent rains were observed, which enhanced the VPD and also leaf development. The Dr_i remained below RAW due to the combination of high precipitation in summer and daily irrigation. Furthermore, frosts after the full bloom with low temperatures < -5 °C occurred. On the contrary, the daily mean water vapor saturation pressure remained above > 0.7 kPa during the full bloom, while steady fluctuation between 0.5 and 0.6 was noted in June and July. The tree water needs rapidly increased at bud break till the canopy was fully developed in June. Moreover, the increase of the temperature and VPD at the beginning of full bloom had as a consequence the rise of ET_a . In parallel, the evaporative demands increased and the days lengthened. During June and July the maximum water demand by the tree took place.

The irrigation thresholds were set by RAW specified according to ECa zone. The ECa values between 2.99 to 4.18 mS m⁻¹ was characterized as low, between 4.18 to 5.33 mS m⁻¹ as mid, between 5.33 to 7.10 mS m⁻¹ as high ECa zone. These zones were used when calculating the water balance. The three classes were applied for compromising readability in the following figures, but also pointing out the differences of tree water needs.

Generally, the rise of temperature and resulting increase of VPD during July and August had as a consequence the escalation of water needs that can be noticed by the increasing thresholds over time (Figs. 6, 7, 8). A decreased level of RAW irrigation threshold was observed from high ECa region, mid irrigation threshold from mid ECa region and enhanced irrigation threshold from low ECa zone (Fig. 6). The RAW irrigation threshold considering the root depth was mainly influenced by the reduced rooting depth compared to the generally assumed 1 m. As a result, the RAW decreased, when

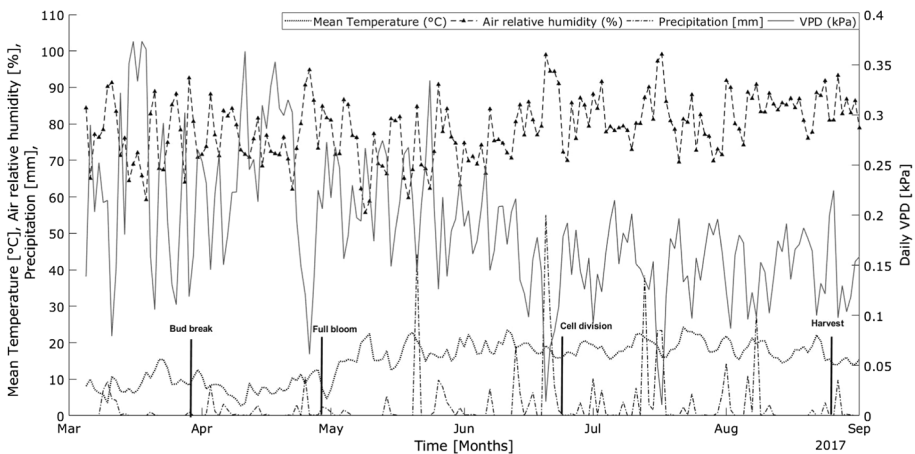


Fig. 5 Daily weather conditions during the cultivation period indicating the phenological stages of the flower and fruit

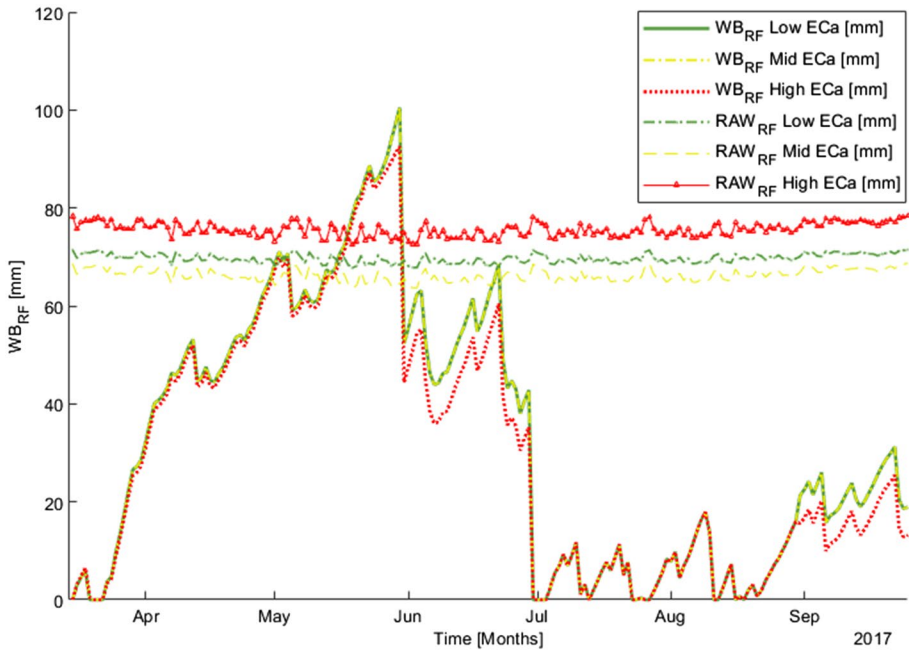


Fig. 6 Daily water balance and readily available water content (RAW) threshold in regions of low, mid and high apparent electrical conductivity of soil (ECa) taking into account the field-uniform root depth of 1 m

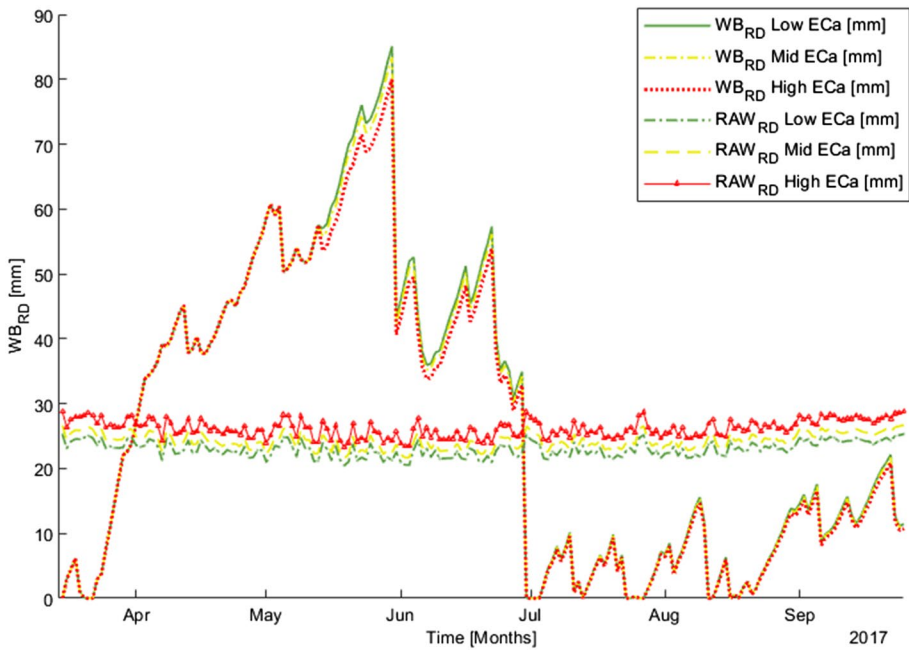


Fig. 7 Daily water balance and readily available water content (RAW) threshold in regions of low, mid and high apparent electrical conductivity of soil (ECa) taking into account the measured root depth ($n=40$) in each region

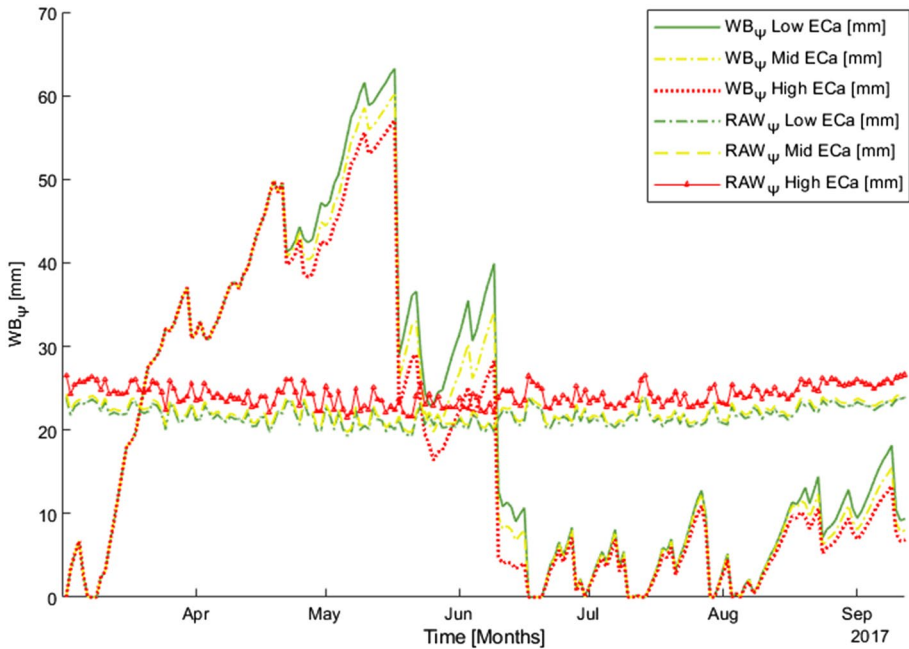


Fig. 8 Daily water balance and readily available water content (RAW) in regions of low, mid and high apparent electrical conductivity of soil (ECa) taking into account the measured root depth ($n=40$) and root water potential ($n=20$) in each region

considering the actual root depth, pointing to enhanced water needs of the fruit trees grown on the widely used M9 rootstock.

Fouli et al. (2012), following the same methodology in crop and soybean suggested that the adjusted root depth can lower the RAW threshold. However, drip irrigation can enhance the rooting density or depth, enabling plants to absorb greater quantities of water and nutrients (Chilundo et al. 2017).

Interestingly, the RAW considering the root depth appeared marginally dependent on the soil texture, since the roots adapt with deeper roots in locations with reduced water holding capacity. Consequently, no difference was found when calculating the RAW for ECa low, mid, and high (Fig. 7).

In addition, including the root water potential at the effective wilting point had only slight impact on the RAW irrigation threshold, which is consistent with low correlation of ECa and root water potential (Fig. 8).

Water balance

The average soil water balance was calculated for each month. During July and August the lowest variance was illustrated in comparison with the other months with $C.V. = 2.16\%$ and $C.V. = 2.1\%$, respectively (Table 5). This is due to the increase of the temperature, reduced VPD and, as a consequence, the rise of the evapotranspiration. The results from WB_{RF} revealed that the water needs increased mid-April till mid-May considering all three thresholds (Fig. 6), signifying that during bud break and full bloom the trees faced drought stress.

Table 5 Descriptive statistics for monthly water balance (mm) considering measured ($n=40$) root depth (index RD) and constant root depth of 1 m (index RF) for locations in the orchard showing low, mid, and high apparent electrical conductivity of the soil (ECa)

	April _{RF}	May _{RF}	June _{RF}	July _{RF}	August _{RF}	September _{RF}
Low ECa						
Mean	19.68	39.21	19.78	2.85	4.69	6.12
SD	0.77	1.76	2.40	0.09	0.14	0.24
CV %	3.91	4.50	12.11	2.99	2.89	3.88
Mid ECa						
Mean	20.18	40.37	20.92	2.90	4.77	6.28
SD	3.05	3.40	3.31	2.70	2.57	1.38
CV %	15.11	8.41	15.80	93.15	53.87	21.97
High ECa						
Mean	20.74	41.63	15.46	2.96	4.87	6.45
SD	0.27	0.59	0.86	0.03	0.05	0.09
CV %	1.29	1.41	5.54	0.98	0.99	1.36
	April _{RD}	May _{RD}	June _{RD}	July _{RD}	August _{RD}	September _{RD}
Low ECa						
Mean	21.74	44.40	18.43	3.07	5.06	6.79
SD	7.02	10.80	8.87	2.65	4.22	4.47
CV %	32.32	24.32	48.15	86.44	83.44	65.80
Mid ECa						
Mean	21.36	43.59	17.59	3.03	4.99	6.66
SD	6.91	10.79	8.84	2.64	4.19	4.44
CV %	32.36	24.75	50.25	87.05	84.08	66.58
High ECa						
Mean	22.00	45.04	19.73	3.10	5.10	6.87
SD	15.97	10.95	9.18	2.70	4.26	4.52
CV %	72.61	24.32	46.51	87.07	83.53	65.81

Considering the water balance using TAW_{RF} , trees from low ECa areas showed the highest water needs, reaching a maximum of 100 mm and mean of 42 mm in May (Table 5). In June the water needs decreased due to the increase of precipitation events in the summer rain climate.

However, Ferreira (2017), pointed out that woody plants adapt to soil conditions, and the modelling of water balance needs to take into account the actual RAW and Ks coefficient for an irrigation scheduling. In the WB_{RD} calculation, considering the soil properties of the field and the measured root depth resulted in increased water needs compared to a water balance estimate assuming field-uniform root depth of 1 m. The root system hardly reached this depth in the present study, and as a result the water supply was limited. Consequently, in the water balance considering the root depth of the trees, high water needs were found from April till mid-June (Fig. 7). In the following months no water stress was revealed due to high precipitation. Kadayifçi et al. (2010) observed the effect of different irrigation system in dwarf apple trees with shallow root. They conclude that the surface irrigation had the highest impact considering the development of the root. Similar results

Table 6 Friedman non parametric analysis among the water balance models (WB) for low, mid, and high ECa (mS/m)

Region	χ^2	Sig.
Low ECa		
WB $_{\psi}$ – WB $_{RD}$	1.14	0.03
WB $_{\psi}$ – WB $_{RF}$	1.86	0.00
WB $_{RD}$ – WB $_{RF}$	0.71	0.18
Mid ECa		
WB $_{\psi}$ – WB $_{RD}$	1.16	0.04
WB $_{\psi}$ – WB $_{RF}$	1.86	0.01
WB $_{RD}$ – WB $_{RF}$	0.92	0.82
High ECa		
WB $_{\psi}$ – WB $_{RD}$	1.21	0.02
WB $_{\psi}$ – WB $_{RF}$	1.79	0.01
WB $_{RD}$ – WB $_{RF}$	0.57	0.28

were found in plum trees (Käthner et al. 2017). In both studies the main root system of the orchard was above 25 cm due to the influence of the dwarfing rootstock, and further exacerbated by drip irrigation which encourages roots to absorb the required water from the top soil. In the present study, high C.V. % were found particularly in the high and mid ECa regions due to smaller differences of root depth measured. However, rooting depth clearly increased in low ECa region. Consequently, the values of WB $_{RD}$ tend to be less dispersed than the FAO model, when considering the spatial variability in the orchard (Table 5). In a study related to wine grapes, it was suggested that the determination of the TAW considering the root depth variation within the field can lead to a more accurate estimation of deficit irrigation requirements and soil water stress (Campos et al. 2016).

Considering the actual water supply by means of the root water potential and root depth, the water needs in WB $_{\psi}$ was still enhanced compared with FAO approach, but decreased (Lauri et al. 2013) compared to the previous model considering only the actual root depth of dwarfing M9 rootstock (Fig. 8). The water balance values point to still considerable water demands between April and May. The water needs were again reduced during the next months due to relatively high precipitation for the region. However, the values of root water potential were highly variable. Green and Clothier (1999) showed that apple tree quickly adjusts the root water uptake in response to changing soil water by increasing uptake from the wet part of the root zone while reducing uptake from the drying part. Under drying conditions the abscisic acid is translocated from roots to leaves, stimulating stomatal closure (Davies et al. 2005). More recent studies confirm morphological adaptations and capability of apple trees to cope with drought stress (Tworkoski et al. 2016).

The daily values from each ECa region were compared for each model by means of Friedman non parametrical analysis (Table 6) (Scheff 2016). The models were compared according the ECa region in the field. The χ^2 depicts the variance of the mean ranks for each ECa zone, the closer to the zero the lower the values were spread. At the level of 0.05 significance, no difference was found between the water balance considering the root depth measured and compared to WB $_{RF}$ in low ($r=0.18$), mid ($r=0.18$) and high ($r=0.29$) ECa regions. On the other hand in the same regions, water balance considering the root depth measured and the water balance considering additionally the wilting point according to the root water potential at the relevant developmental stage of the tree revealed the highest

χ^2 of 1.86, indicating a high variance between the trees. Moreover, in low and mid ECa regions the two models appeared different with $r < 0.01$.

In the present study, the areas with high ECa had a yield of 22–28 kg per tree, while the low ECa areas depicted yields of 18–24 kg per tree. The results indicate that the trees with relatively shallow root and high ECa had slightly enhanced yield, while deeper root systems in low ECa areas had reduced yield. However, the yield was measured for only 15 trees in each zone and yields showed no significant difference by zone. Overall, the impact of soil variability seems to be measurable, while trees were able to cope with variation in soil texture mainly by means of adapted root depth. In an earlier apple orchard study, high electrical conductivities also tended to be related with high silt contents, whereas low conductivities with sand. However, no relationship was revealed between yield and ECa (Aggelopoulou et al. 2013), maybe pointing as well to plant adaptation such as found in the present study.

Conclusion

The outcomes of this study reveal information for the better understanding of soil spatial variability in drip-irrigated apple orchard and its impact on water needs during the vegetation period. The orchard had a light soil profile with high amounts of sand and silt. The dwarfing rootstock resulted in generally shallow root depth, never reaching the depth of 1 m assumed in FAO recommendations.

Through the mapping of ECa, locations of the field were characterized showing similar behaviour in phenotypic adaptation, namely rooting depth, of the apple trees. Figures 2 and 3 show that considerable spatial variation for soil electrical electricity and root depth was present. This spatial variation is relevant for optimizing irrigation schedules. The trees coped with the decreased water supply in sandy zones by means of this adaptation and, as a result, the RAW irrigation threshold was reached to a lesser extend than without the adaptation.

Furthermore, ECa had a positive correlation with root water potential in full bloom and at harvest during dawn, an observation that may point to an expected adjustment of root water potential serving as an adaptation tool by the tree to cope with reduced water supply. However, no differences were found for low and high ECa locations compared in the orchard. The approach may be more relevant for rain fed fruit production. The impact of plant response on the RAW irrigation threshold and water balance resulted in highly different water needs as shown in Figs. 6, 7, 8. Thus the spatial resolution of irrigation should be approached in orchards considering the plant responses.

Funding Funding was supported by EIP-AGRI, ILB, Ministerium für Ländliche Entwicklung, Umwelt und Landwirtschaft (MLUL) Brandenburg, (Grant no. 2045).

References

- Aggelopoulou, K., Castrignanò, A., Gemtos, T., & De Benedetto, D. (2013). Delineation of management zones in an apple orchard in Greece using a multivariate approach. *Computers and Electronics in Agriculture*, 90, 119–130. <https://doi.org/10.1016/j.compag.2012.09.009>.

- Alexandridis, T. K., Panagopoulos, A., Galanis, G., Alexiou, I., Cherif, I., Chemin, Y., ... Zalidis, G. C. (2014). Combining remotely sensed surface energy fluxes and GIS analysis of groundwater parameters for irrigation system assessment. *Irrigation Science*, 32(2), 127–140. <https://doi.org/10.1007/s00271-013-0419-8>.
- Allen, R. G., Pereira, L. S., Raes, D., & Smith, M. (1998). Crop evapotranspiration—guidelines for computing crop water requirements-FAO Irrigation and Drainage Paper 56. FAO, Rome, 300(9), D05109.
- Allen, R. G., Pereira, L. S., Smith, M., Raes, D., & Wright, J. L. (2005). FAO-56 dual crop coefficient method for estimating evaporation from soil and application extensions. *Journal of Irrigation and Drainage Engineering*, 131(1), 2–13. [https://doi.org/10.1061/\(ASCE\)0733-9437\(2005\)131:1\(2\)](https://doi.org/10.1061/(ASCE)0733-9437(2005)131:1(2)).
- Auernhammer, H. (2001). Precision farming—the environmental challenge. *Computers and Electronics in Agriculture*, 30(1–3), 31–43. [https://doi.org/10.1016/S0168-1699\(00\)00153-8](https://doi.org/10.1016/S0168-1699(00)00153-8).
- Blackmore, S., Godwin, R. J., & Fountas, S. (2003). The analysis of spatial and temporal trends in yield map data over six years. *Biosystems Engineering*, 84(4), 455–466. [https://doi.org/10.1016/S1537-5110\(03\)00038-2](https://doi.org/10.1016/S1537-5110(03)00038-2).
- Blum, A. (2017). Osmotic adjustment is a prime drought stress adaptive engine in support of plant production. *Plant, Cell and Environment*, 40(1), 4–10. <https://doi.org/10.1111/pce.12800>.
- Cambardella, C. A., Moorman, T. B., Novak, J. M., Parkin, T. B., Karlen, D. L., Turco, R. F., et al. (1994). Field-scale variability of soil properties in Central Iowa soils. *Soil Science Society of America Journal*, 58, 1501–1511.
- Campos, I., González-Piqueras, J., Carrara, A., Villodre, J., & Calera, A. (2016). Estimation of total available water in the soil layer by integrating actual evapotranspiration data in a remote sensing-driven soil water balance. *Journal of Hydrology*, 534, 427–439. <https://doi.org/10.1016/j.jhydrol.2016.01.023>.
- Carsel, R. F., & Parrish, R. S. (1988). Developing joint probability distributions of soil water retention characteristics. *Water Resources Research*, 24(5), 755–769. <https://doi.org/10.1029/WR024i005p00755>.
- Chilundo, M., Joel, A., Wesström, I., Brito, R., & Messing, I. (2017). Response of maize root growth to irrigation and nitrogen management strategies in semi-arid loamy sandy soil. *Field Crops Research*, 200, 143–162. <https://doi.org/10.1016/j.fcr.2016.10.005>.
- Corwin, D. L., & Lesch, S. M. (2013). Protocols and guidelines for field-scale measurement of soil salinity distribution with ECa-directed soil sampling. *Journal of Environmental and Engineering Geophysics*, 18(1), 1–25. <https://doi.org/10.2113/JEEG18.1.1>.
- Corwin, D. L., & Plant, R. E. (2005). Applications of apparent soil electrical conductivity in precision agriculture. *Computers and Electronics in Agriculture*, 46, 1–3. <https://doi.org/10.1016/j.compag.2004.10.004>.
- Courault, D., Seguin, B., & Olioso, A. (2005). Review on estimation of evapotranspiration from remote sensing data: from empirical to numerical modeling approaches. *Irrigation and Drainage Systems*, 19(3–4), 223–249.
- Daccache, A., Ciurana, J. S., Diaz, J. R., & Knox, J. W. (2014). Water and energy footprint of irrigated agriculture in the Mediterranean region. *Environmental Research Letters*, 9(12), 124014. <https://doi.org/10.1088/1748-9326/9/12/124014>.
- Davies, W. J., Kudoyarova, G., & Hartung, W. (2005). Long-distance ABA signaling and its relation to other signaling pathways in the detection of soil drying and the mediation of the plant's response to drought. *Journal of Plant Growth Regulation*, 24(4), 285. <https://doi.org/10.1007/s00344-005-0103-1>.
- Dodd, I. C., Egea, G., Watts, C. W., & Whalley, W. R. (2010). Root water potential integrates discrete soil physical properties to influence ABA signalling during partial rootzone drying. *Journal of Experimental Botany*, 61(13), 3543–3551. <https://doi.org/10.1093/jxb/erq195>.
- Fernandez, R. T., Perry, R. L., & Ferree, D. C. (1995). Root distribution patterns of nine apple rootstock in two contrasting soil types. *Journal of the American Society for Horticultural Science*, 120(1), 6–13.
- Ferree, D. C., & Streeter, J. G. (2004). Response of container-grown grapevines to soil compaction. *HortScience*, 39(6), 1250–1254.
- Ferreira, M. I. (2017). Stress coefficients for soil water balance combined with water stress indicators for irrigation scheduling of woody crops. *Horticulturae*, 3(2), 38. <https://doi.org/10.3390/horticulturae3020038>.
- Fouli, Y., Duiker, S. W., Fritton, D. D., Hall, M. H., Watson, J. E., & Johnson, D. H. (2012). Double cropping effects on forage yield and the field water balance. *Agricultural Water Management*, 115, 104–117. <https://doi.org/10.1016/j.agwat.2012.08.014>.
- Green, S. R., & Clothier, B. E. (1999). The rootzone dynamics of water uptake by a mature apple tree. *Plant and Soil*, 206, 61–77. <https://doi.org/10.1023/A:1004368906698>.
- Green, S. R., Vogeler, I., Clothier, B. E., Mills, T. M., & Van Den Dijssel, C. (2003). Modelling water uptake by a mature apple tree. *Soil Research*, 41(3), 365–380. <https://doi.org/10.1071/SR02129>.

- Haberle, J., & Svoboda, P. (2015). Calculation of available water supply in crop root zone and the water balance of crops. *Contributions to Geophysics and Geodesy*, 45(4), 285–298. <https://doi.org/10.1515/congeo-2015-0025>.
- Haghverdi, A., Leib, B. G., Washington-Allen, R. A., Ayers, P. D., & Buschermohle, M. J. (2015). Perspectives on delineating management zones for variable rate irrigation. *Computers and Electronics in Agriculture*, 117, 154–167. <https://doi.org/10.1016/j.compag.2015.06.019>.
- Hedley, C. B., Bradbury, S., Ekanayake, J., Yule, I. J., & Carrick, S. (2010, November). Spatial irrigation scheduling for variable rate irrigation. In *Proceedings of the New Zealand Grassland Association* (Vol. 72, pp. 97–102). New Zealand Grassland Association.
- Hedley, C. B., & Yule, I. J. (2009). A method for spatial prediction of daily soil water status for precise irrigation scheduling. *Agricultural Water Management*, 96(12), 1737–1745. <https://doi.org/10.1016/j.agwat.2009.07.009>.
- Herppich, W. B., & Geyer, M. (2001). Osmotic and elastic adjustment, and product quality in cold-stored carrot roots (*Daucus carota* L.). *Gartenbauwissenschaft*, 66(1), 20–26.
- Hezarjaribi, A., & Sourell, H. (2007). Feasibility study of monitoring the total available water content using non-invasive electromagnetic induction-based and electrode-based soil electrical conductivity measurements. *Irrigation and Drainage: The Journal of the International Commission on Irrigation and Drainage*, 56(1), 53–65. <https://doi.org/10.1002/ird.289>.
- Horney, R. D., Taylor, B., Munk, D. S., Roberts, B. A., Lesch, S. M., & Plant, R. E. (2005). Development of practical site-specific management methods for reclaiming salt-affected soil. *Computers and Electronics in Agriculture*, 46(1–3), 379–397. <https://doi.org/10.1016/j.compag.2004.11.008>.
- Humphreys, M. T., Raun, W. R., Martin, K. L., Freeman, K. W., Johnson, G. V., & Stone, M. L. (2005). Indirect estimates of soil electrical conductivity for improved prediction of wheat grain yield. *Communications in Soil Science and Plant Analysis*, 35(17–18), 2639–2653. <https://doi.org/10.1081/LCSS-200030421>.
- Hunink, J. E., Contreras, S., Soto-García, M., Martín-Gorriz, B., Martínez-Álvarez, V., & Baille, A. (2015). Estimating groundwater use patterns of perennial and seasonal crops in a Mediterranean irrigation scheme, using remote sensing. *Agricultural Water Management*, 162, 47–56. <https://doi.org/10.1016/j.agwat.2015.08.003>.
- Hunsaker, D. J., French, A. N., Waller, P. M., Bautista, E., Thorp, K. R., Bronson, K. F., et al. (2015). Comparison of traditional and ET-based irrigation scheduling of surface-irrigated cotton in the arid southwestern USA. *Agricultural Water Management*, 159, 209–224. <https://doi.org/10.1016/j.agwat.2015.06.016>.
- Hurley, M. B., & Rowarth, J. S. (1999). Resistance to root growth and changes in the concentrations of ABA within the root and xylem sap during root-restriction stress. *Journal of Experimental Botany*, 50(335), 799–804. <https://doi.org/10.1093/jxb/50.335.799>.
- Jensen, M. E., Burman, R. D., & Allen, R. G. (1990). Evaporation and irrigation water requirements. ASCE Manuals and Reports on Eng. Practices No. 70, New York.
- Kadayifçi, A., Öz, H., & Atilgan, A. (2010). The effects of different irrigation methods on root distribution, intensity and effective root depth of young dwarf apple trees. *African Journal of Biotechnology*, 9(27), 4217–4224.
- Käthner, J., Ben-Gal, A., Gebbers, R., Peeters, A., Herppich, W. B., & Zude-Sasse, M. (2017). Evaluating spatially resolved influence of soil and tree water status on quality of European plum grown in semi-humid climate. *Frontiers in Plant Science*, 8, 1053. <https://doi.org/10.3389/fpls.2017.01053>.
- Lauri, P. É., Marceron, A., Normand, F., Dambreville, A., & Regnard, J. L. (2013). Soil water deficit decreases xylem conductance efficiency relative to leaf area and mass in the apple. *Journal of Plant Hydraulics*, 1, e0003.
- Levin, I., Assaf, R., & Bravdo, B. (1979). Soil moisture and root distribution in an apple orchard irrigated by tricklers. *Plant and Soil*, 52(1), 31–40.
- Lo, T. H., Heeren, D. M., Mateos, L., Luck, J. D., Martin, D. L., Miller, K. A., ... Shaver, T. M. (2017). Field characterization of field capacity and root zone available water capacity for variable rate irrigation. *Applied Engineering in Agriculture*, 33(4), 559–572. <https://doi.org/10.13031/aea.11963>.
- McCutcheon, M. C., Farahani, H. J., Stednick, J. D., Buchleiter, G. W., & Green, T. R. (2006). Effect of soil water on apparent soil electrical conductivity and texture relationships in a dryland field. *Bio-systems Engineering*, 94(1), 19–32. <https://doi.org/10.1016/j.biosystemseng.2006.01.002>.
- Moral, F. J., Terrón, J. M., & Rebollo, F. J. (2011). Site-specific management zones based on the Rasch model and geostatistical techniques. *Computers and Electronics in Agriculture*, 75(2), 223–230. <https://doi.org/10.1016/j.still.2009.12.002>.

- Naor, A., Gal, Y., & Peres, M. (2006). The inherent variability of water stress indicators in apple, nectarine and pear orchards, and the validity of a leaf-selection procedure for water potential measurements. *Irrigation Science*, 24(2), 129–135. <https://doi.org/10.1007/s00271-005-0016-6>.
- Naor, A., Klein, I., Hupert, H., Grinblat, Y., Peres, M., & Kaufman, A. (1999). Water stress and crop level interactions in relation to nectarine yield, fruit size distribution, and water potentials. *Journal of the American Society for Horticultural Science*, 124(2), 189–193.
- Oldoni, H., & Bassoi, L. H. (2016). Delineation of irrigation management zones in a quartzsammment of the Brazilian semi-arid region. *Pesquisa Agropecuária Brasileira*, 51(9), 1283–1294. <https://doi.org/10.1590/s0100-204x2016000900028>.
- Paço, T. A., Ferreira, M. I., Rosa, R. D., Paredes, P., Rodrigues, G. C., Conceição, N., ... Pereira, L. S. (2012). The dual crop coefficient approach using a density factor to simulate the evapotranspiration of a peach orchard: SIMDualKc model versus eddy covariance measurements. *Irrigation Science*, 30(2), 115–126. <https://doi.org/10.1007/s00271-011-0267-3>.
- Panagopoulos, T., Jesus, J., Antunes, M. D. C., & Beltrao, J. (2006). Analysis of spatial interpolation for optimizing management of a salinized field cultivated with lettuce. *European Journal of Agronomy*, 24(1), 1–10. <https://doi.org/10.1016/j.eja.2005.03.001>.
- Pathak, H. S., Brown, P., & Best, T. (2019). A systematic literature review of the factors affecting the precision agriculture adoption process. *Precision Agriculture*. <https://doi.org/10.1007/s11119-019-09653-x>.
- Peeters, A., Zude, M., Käthner, J., Ünlü, M., Kanber, R., Hetzroni, A., ... Ben-Gal, A. (2015). Getis-Ord's hot-and cold-spot statistics as a basis for multivariate spatial clustering of orchard tree data. *Computers and Electronics in Agriculture*, 111, 140–150. <https://doi.org/10.1016/j.compag.2014.12.011>.
- Pereira, L. S., Allen, R. G., Smith, M., & Raes, D. (2015). Crop evapotranspiration estimation with FAO56: Past and future. *Agricultural Water Management*, 147, 4–20. <https://doi.org/10.1016/j.agwat.2014.07.031>.
- Pérez-Pastor, A., Ruiz-Sánchez, M. C., & Domingo, R. (2014). Effects of timing and intensity of deficit irrigation on vegetative and fruit growth of apricot trees. *Agricultural Water Management*, 134, 110–118. <https://doi.org/10.1016/j.agwat.2013.12.007>.
- Phogat, V., Skewes, Mark A., Mahadevan, M., et al. (2013). Evaluation of soil plant system response to pulsed drip irrigation of an almond tree under sustained stress conditions. *Agricultural Water Management*, 118, 1–11. <https://doi.org/10.1016/j.agwat.2012.11.015>.
- Puértolas, J., Conesa, M. R., Ballester, C., & Dodd, I. C. (2014). Local root abscisic acid (ABA) accumulation depends on the spatial distribution of soil moisture in potato: implications for ABA signalling under heterogeneous soil drying. *Journal of Experimental Botany*, 66(8), 2325–2334. <https://doi.org/10.1093/jxb/eru501>.
- Rodríguez-Pérez, J. R., Plant, R. E., Lambert, J. J., & Smart, D. R. (2011). Using apparent soil electrical conductivity (ECa) to characterize vineyard soils of high clay content. *Precision Agriculture*, 12(6), 775–794. <https://doi.org/10.1007/s11119-011-9220-y>.
- Scheff, S. W. (2016). *Fundamental statistical principles for the neurobiologist: A survival guide*. Academic Press. <https://doi.org/10.1016/C2015-0-02471-6>.
- Shaner, D. L., Khosla, R., Brodahl, M. K., Buchleiter, G. W., & Farahani, H. J. (2008). How well does zone sampling based on soil electrical conductivity maps represent soil variability? *Agronomy Journal*, 100(5), 1472–1480. <https://doi.org/10.2134/agronj2008.0060>.
- Sponagel, H., Grotenthaler, W., Hartmann, K. J., Hartwich, R., Jaentzko, P., Joisten, H., Kühn, D., Sabel, K.J., Traidel, R. (2005). *Bodenkundliche Kartieranleitung*. Bundesanstalt für Geowissenschaften und Rohstoffe und den Geologischen Landesämtern in der Bundesrepublik Deutschland Hannover. <https://doi.org/10.1017/cbo9781107415324.004>.
- Sudduth, K. A. (1999). Engineering technologies for precision farming. *International seminar on agricultural mechanization technology for precision farming* (pp. 5–27). Rural Development Admin: Suwon.
- Sudduth, K. A., Kitchen, N. R., Wiebold, W. J., Batchelor, W. D., Bollero, G. A., Bullock, D. G., ... Thelen, K. D. (2005). Relating apparent electrical conductivity to soil properties across the north-central USA. *Computers and Electronics in Agriculture*, 46(1–3), 263–283. <https://doi.org/10.1016/j.compag.2004.11.010>.
- Taubner, H., Roth, B., & Tippkötter, R. (2009). Determination of soil texture: Comparison of the sedimentation method and the laser-diffraction analysis. *Journal of Plant Nutrition and Soil Science*, 172(2), 161–171. <https://doi.org/10.1002/jpln.200800085>.

- Tombesi, S., Johnson, R. S., Day, K. R., & DeJong, T. M. (2009). Relationships between xylem vessel characteristics, calculated axial hydraulic conductance and size-controlling capacity of peach rootstocks. *Annals of Botany*, *105*(2), 327–331.
- Trought, M. C., & Bramley, R. G. (2011). Vineyard variability in Marlborough, New Zealand: characterising spatial and temporal changes in fruit composition and juice quality in the vineyard. *Australian Journal of Grape and Wine Research*, *17*(1), 79–89. <https://doi.org/10.1111/1/j.1755-0238.2010.00120.x>.
- Turner, N. C. (1988). Measurement of plant water status by the pressure chamber technique. *Irrigation Science*, *9*(4), 289–308.
- Twoorkoski, T., Fazio, G., & Glenn, D. M. (2016). Apple rootstock resistance to drought. *Scientia Horticulturae*, *204*, 70–78. <https://doi.org/10.1016/j.scienta.2016.01.047>.
- van Genuchten, M. T., & Pachepsky, Y. A. (2011). Hydraulic properties of unsaturated soils. In *Encyclopedia of agrophysics* (pp. 368–376). Dordrecht: Springer. https://doi.org/10.1007/978-90-481-3585-1_69.
- Verstraeten, W. W., Veroustraete, F., & Feyen, J. (2008). Assessment of evapotranspiration and soil moisture content across different scales of observation. *Sensors*, *8*(1), 70–117. <https://doi.org/10.3390/s8010070>.
- Watson, T. W., Appel, N. D., Arnold, A. M., & Kenerley, M. C. (2006). Spatial distribution of Malus root systems in irrigated, trellised orchards. *The Journal of Horticultural Science & Biotechnology*, *81*(4), 745–753. <https://doi.org/10.1080/14620316.2006.11512132>.
- Whitmore, A. P., & Whalley, W. R. (2009). Physical effects of soil drying on roots and crop growth. *Journal of Experimental Botany*, *60*(10), 2845–2857. <https://doi.org/10.1093/jxb/erp200>.
- Zude-Sasse, M., Fountas, S., Gemtos, T. A., & Abu-Khalaf, N. (2016). Applications of precision agriculture in horticultural crops. *European Journal for Horticultural Science*, *81*(2), 78–90. <https://doi.org/10.17660/ejhs.2016/81.2.2>.

Publisher's Note Springer Nature remains neutral with regard to jurisdictional claims in published maps and institutional affiliations.